Proceedings of the
Annual Stability Conference
Structural Stability Research Council
Louisville, Kentucky, April 13-16, 2021

Unfavorable imperfection shapes in steel plate girders for web local crippling

Sasa Kovacevic[1], Nenad Markovic[2], Aleksandar Ceranic[3], Milica Bendic[4]

Abstract

The paper reports a numerical investigation and determination of unfavorable geometric imperfection shapes in steel plate girders subjected to concentrated compressive forces by means of the ultimate limit state. This load case is present in many engineering applications, including beam-beam and beam-column connections, deep crane runway beams loaded by crane wheels, and during the incremental launching of multi-span steel and composite bridges over temporary or permanent supports. A parametric imperfection-sensitivity study has been performed on I-shaped steel plate girders employing geometrically and materially nonlinear finite element analysis. Experimentally measured, buckling mode-affine, and hand defined sinusoidal geometric imperfections were varied in the study in combination with varying patch load lengths and relative stiffnesses of the longitudinal stiffener. It is shown in the paper that geometric imperfections can play a decisive role and significantly affect the ultimate strength of longitudinally unstiffened and stiffened steel plate girders. Unfavorable geometric imperfection shapes in steel plate girders subjected to edge loading are governed by the patch load length and the relative stiffness of the longitudinal stiffener. Different unfavorable geometric imperfections were found for different patch load lengths and relative stiffnesses. Local geometric imperfections defined in the upper web sub-panel yield lower ultimate strengths than global geometric imperfections (defined over the whole web depth). The lowest ultimate strengths were returned for geometric imperfections that resembled the deformation at collapse (collapse-affine imperfections). Further research should focus on finding an *equivalent shape* that resembles the deformation at failure for different patch load lengths and girder characteristics.

1. Introduction

Steel plate girders can support greater loads on longer spans, which cannot be economically carried by standard rolled beams or trusses. Besides a myriad of advantages, one of the most important demerits of the steel plate girders is susceptibility to lateral buckling. To prevent web buckling, steel plate girders are usually reinforced with stiffening members, which proves to be a more economical approach than using a stockier web. The current AISC Specification (ANSI/AISC 2016) and European design standard (EN 1993-1-5 2006) require a stability control check for concentrated compressive forces (patch loading). This load case is present in many

[1] Graduate Research and Teaching Assistant, Washington State University, <sasa.kovacevic@wsu.edu>
[2] Assistant Professor, University of Belgrade, <nenad@grf.bg.ac.rs>
[3] MSc, Spenncon AS, <ceranicaleksandar@gmail.com>
[4] Graduate Teaching Assistant, University of Belgrade, <milicabendic95@gmail.com>

applications, including beam-beam and beam-column connections as well as deep crane runway beams loaded by crane wheels. The most realistic load case is during the incremental launching of multi-span steel and composite bridges over temporary or permanent supports. It has been observed experimentally that the ultimate carrying patch load capacity is achieved after local web buckling and deformation of the loaded flange in the vicinity of the point of loading (Bergfelt 1983), (Janus et al. 1988), (Markovic & Hajdin 1992), (Markovic 2003), (Kovesdi et al. 2018), (Markovic & Kovacevic 2019), and (Kovacevic & Markovic 2020). Two typical failure modes for longitudinally unstiffened and stiffened steel plate girders subjected to patch loading are shown in Fig. 1.

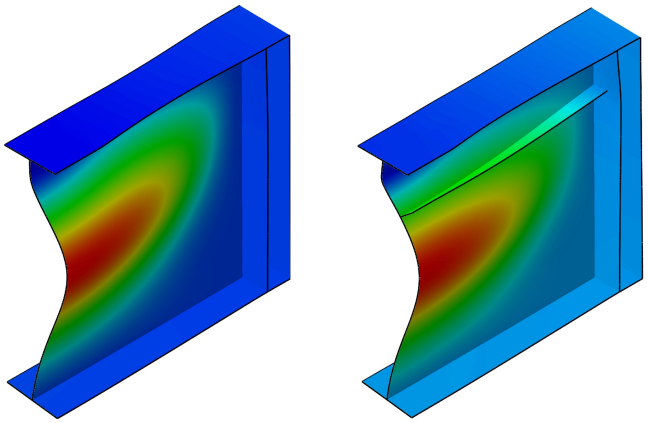

Figure 1: Typical failure modes for longitudinally unstiffened and stiffened steel plate girders subjected to patch loading.

Chapter J of the latest edition of the AISC Specification (ANSI/AISC 2016) provides formulas for predicting the strength of unstiffened webs and webs with vertical stiffeners under local compressive loads. The current European design standard (EN 1993-1-5 2006) gives guidance for both longitudinally unstiffened and stiffened webs under edge loading. Comparing the experimentally obtained ultimate strengths of longitudinally unstiffened steel plate girders with both standards, one can observe that the standards underestimate the ultimate strength, especially for longer patch load lengths, Fig 2. Moreover, as observed in Fig. 2, the AISC Specification returns less conservative ultimate strengths than the EN 1993-1-5 standard.

In order to decrease this gap between the experimentally obtained ultimate strengths and ones predicted by the design standards, designers can employ the finite element analysis for the ultimate limit state, as allowed by the EN 1993-1-5 standard. The essential data for an adequate ultimate limit state design comprises information on unavoidable geometric and structural imperfections (residual stresses). Both standards state that a chosen imperfection should yield the lowest resistance (in direct modeling of imperfection or numerical analysis). However, the design standards lack information on these imperfections, and no specific geometric shape or stress pattern is provided. Structural imperfections do not significantly influence the ultimate strength of steel plate girders under patch loading (Chacon et a. 2009) (Chacon et al. 2012); thus, they can be excluded from the analysis. The usual practice for geometric imperfections is to use buckling mode-affine or hand-defined sinusoidal geometric imperfections, approaches frequently used in the literature (Kovesdi et al. 2018), (Davaine 2005), (Chacon et al. 2009), (Graciano et al. 2011), (Kovesdi 2018), (Loaiza et al. 2018), (Kovacevic et al. 2019), (Kovacevic & Markovic

2019), (Demari et al. 2020). Hence, it is not clear from the patch loading point of view, which imperfections lead to the lowest ultimate strength.

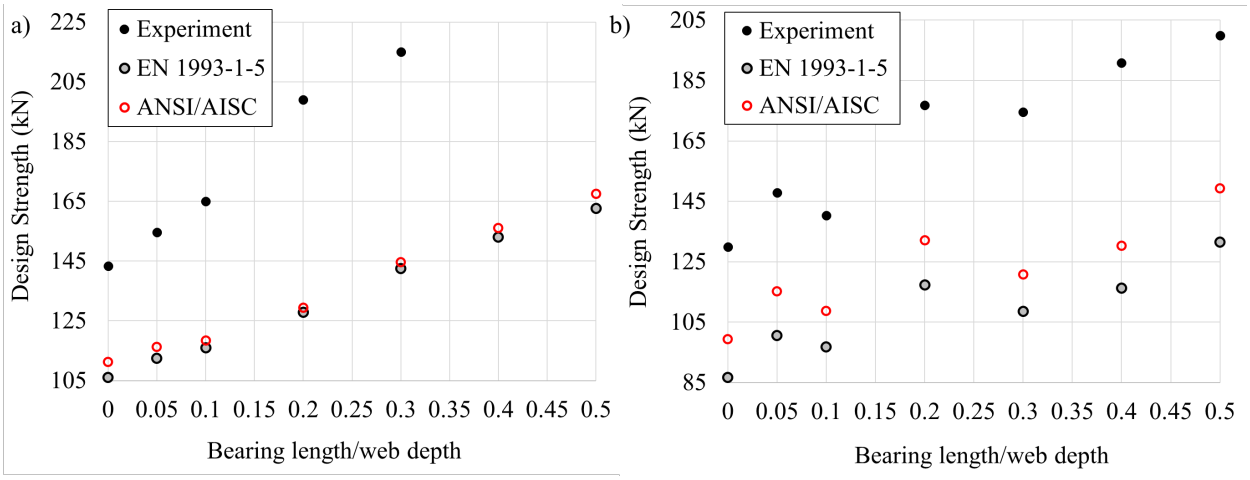

Figure 2: Ultimate strength of longitudinally unstiffened steel plate girders determined by the design standards (ANSI/AISC 2016), (EN 1993-1-5 2006) and experimentally (a) (Markovic & Kovacevic 2019); (b) (Kovacevic & Markovic 2020). Refer to Fig. 3 for general notation.

The main objective of this study is to determine unfavorable imperfection shapes in steel plate girders subjected to edge loading. The present paper encapsulates our previous numerical studies (Hajdin et al. 2019), (Kovacevic & Markovic 2019), (Kovacevic et al. 2019), (Kovacevic et al. 2021a), and (Kovacevic et al. 2021b) on the imperfection sensitivity of steel plate girders to geometric imperfections in combination with varying patch load lengths and relative stiffnesses of the longitudinal stiffener.

2. Parametric study

The present finite element parametric study was designed to determine the influence of various geometric imperfections (in combination with various patch load lengths) on the patch load resistance of I-shaped steel plate girders. The patch load length, s_s, was varied from $s_s/h_w = 0.01$ to $s_s/h_w = 0.50$, while geometric imperfections included the experimentally measured imperfections (Kovacevic & Markovic 2020), buckling mode-affine, and hand-defined sinusoidal imperfections. The geometric imperfections considered were defined similarly to those in our previous numerical analyses (Kovacevic et al. 2019), (Kovacevic & Markovic 2019), and (Hajdin et al. 2019) in which steel plate girders with a web panel aspect ratio of 1 were used; thus, a direct comparison could be made between these analyses.

A short description of the finite element model employed in the current parametric study is given in the following subsections, while the interested reader is referred to (Kovacevic et al. 2021b) for more details. The numerical model was validated juxtaposing the experimentally measured and numerically evaluated path load resistances.

2.1 Girder geometry

The geometry of the girders considered is based on the experimental investigation (Kovacevic & Markovic 2020) conducted on I-shaped steel plate girders. The following girder dimensions were used: web thickness $t_w = 4$ mm, flange thickness $t_f = 8$ mm, web depth $h_w = 500$ mm, girder span

a = 1000 mm (web panel aspect ratio a/h_w = 2), and flange width b_f = 120 mm. The thickness of the transverse stiffeners at both ends was 8 mm. Refer to Fig. 3 for plate girder notation.

Two different flat longitudinal stiffeners were employed: a relatively *weak* longitudinal stiffener with relative stiffness $\gamma_s = 21.67$ (h_s = 30 mm and t_s = 8 mm - originally used in experimental investigations (Markovic & Kovacevic 2019) and (Kovacevic & Markovic 2020)), and a relatively *strong* longitudinal stiffener with relative stiffness $\gamma_s = 103.46$ (h_s = 55 mm and t_s = 8 mm). The longitudinal stiffeners were placed at one-fifth of the girder depth ($b_1 = 0.2h_w$), the optimum location for the flexural and shear resistance (Cooper 1965). The relative flexural stiffness of the longitudinal stiffener γ_s can be defined according to (EN 1993-1-5 2006).

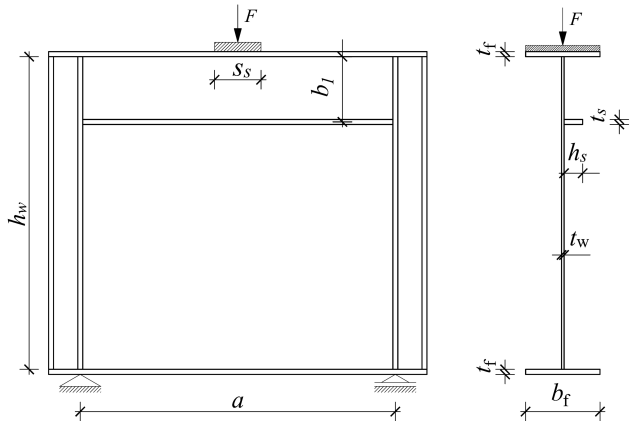

Figure 3: Longitudinally stiffened plate girder under transverse concentrated loading, general notation.

2.2 Finite element mesh

To build the girder geometry and create a numerical model, the commercial multi-purpose finite element software Abaqus was employed (Abaqus Simulia 2016).). The girders were modeled in real size using fully integrated four-node quadrilateral shell elements (S4) from the Abaqus element library. This finite element is applicable for most thick and thin shell applications with large strains. A very finely structured finite element mesh was applied to all the girders with quadrilateral elements only, Fig. 4. Based on an *h*-refinement analysis (Kovacevic et al. 2019), a global element size of 5 mm was adopted for this study. The numerical models contained approximately 260,000 and 266,000 degrees of freedom for longitudinally unstiffened and stiffened plate girders, respectively.

2.3 Boundary and loading conditions

The girders were modeled as simply supported (preventing vertical displacement and displacement perpendicular to the plane of the web panel) at the transverse stiffeners. These boundary conditions correspond to the experimental setup used in (Markovic & Kovacevic 2019) and (Kovacevic & Markovic 2020). The rigid loading blocks were modeled as separate structural elements, and applied loads were transferred through these elements onto the upper flange, Fig. 4. The central node of the loading blocks was defined as the master node, while the corresponding nodes on the loaded flange were defined as slave nodes. The displacement-controlled approach was applied, accompanied by a small compressive displacement applied to the master node. To simulate real loading conditions as in the experiments (Markovic &

Kovacevic 2019) and (Kovacevic & Markovic 2020), all degrees of freedom of the master node were restricted except in the vertical direction. The structural interaction between the loading blocks and the loaded flange was defined through the contact interface.

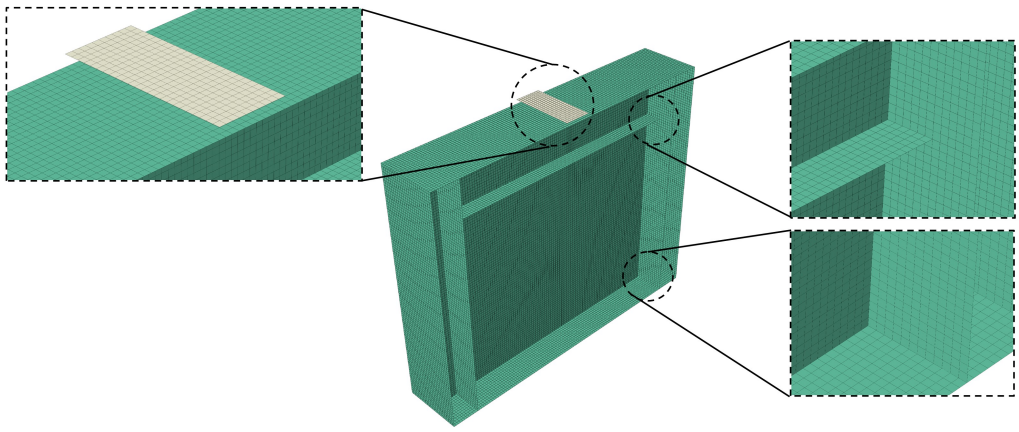

Figure 4: Finite element mesh and rigid loading blocks.

2.4 Material properties

The patch load resistance was determined using geometrically and materially nonlinear analysis. The modified Riks method (Riks 1979) was applied to trace the complex nonlinear load-displacement response of the girders. The material was incorporated into the numerical model as isotropic material with the isotropic work hardening assumption using material data obtained from standard tensile tests. The material properties of the web panel and flanges were adopted from (Markovic & Kovacevic 2019) with the web panel yield stress f_{yw} = 323 MPa and flange yield stress f_{yf} = 322 MPa accompanying the stress-strain curves given in Fig. 5. In addition to this, Young's modulus of 205 GPa and Poisson's ratio of 0.3 were employed to define the elastic behavior of the girders.

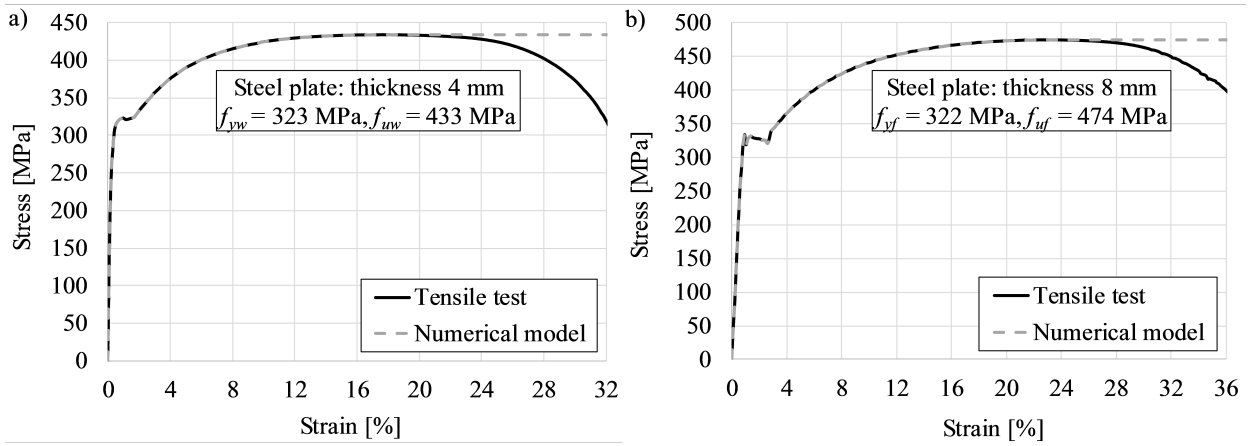

Figure 5: Engineering stress-strain curves obtained by tensile test vs. curves used in the simulations for: (a) web panel. (b) Flanges, transverse and longitudinal stiffeners.

2.5 Geometric imperfections

One of the most popular approaches to introduce geometric imperfections into nonlinear finite element analysis (FEA) is to use buckling mode shapes (obtained from an eigenvalue analysis). The same method was followed in this study, and the first three buckling mode shapes, as well as

their combination, were examined in the present numerical analysis. Representative shapes of the first three buckling modes are shown in Fig. 6, Fig. 7, and Fig. 8. All the buckling mode shapes illustrated in these figures are valid for all the patch load lengths considered ($s_s/h_w \leq 0.50$) except for the third buckling mode shape of longitudinally stiffened steel plate girders, which is an asymmetric buckling mode shape for applied patch load lengths $s_s/h_w \geq 0.30$ and $s_s/h_w \geq 0.15$ in the cases of $\gamma_s = 21.67$ and $\gamma_s = 103.46$, respectively (Fig. 8 and Fig. 9).

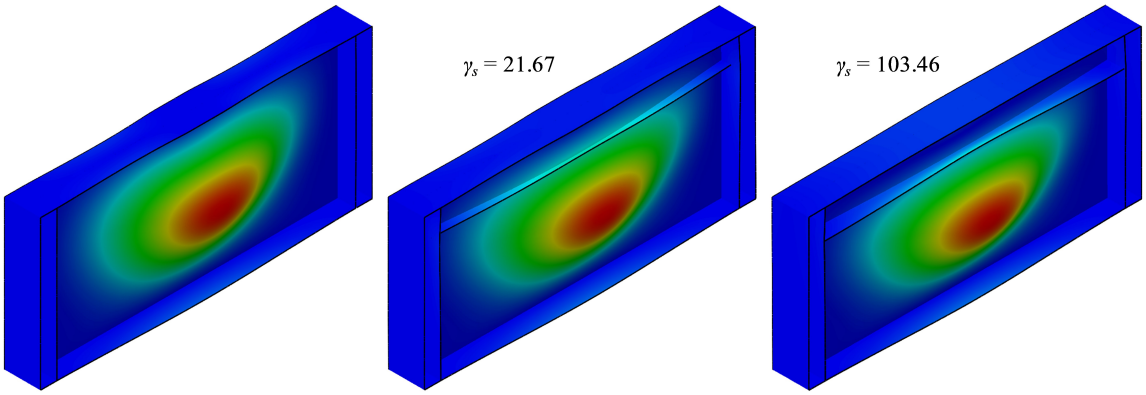

Figure 6: First buckling mode of longitudinally unstiffened and stiffened steel plate girders for all patch load lengths considered ($s_s/h_w \leq 0.50$).

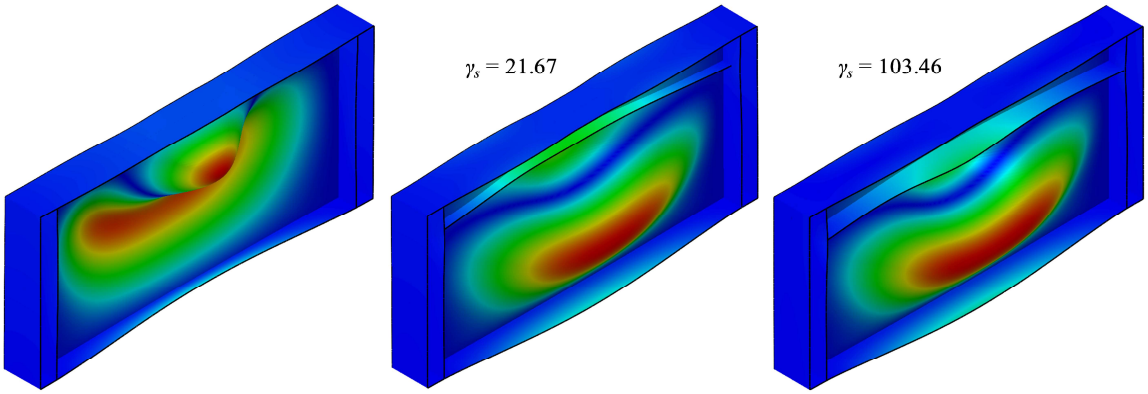

Figure 7: Second buckling mode of longitudinally unstiffened and stiffened steel plate girders for all patch load lengths considered ($s_s/h_w \leq 0.50$).

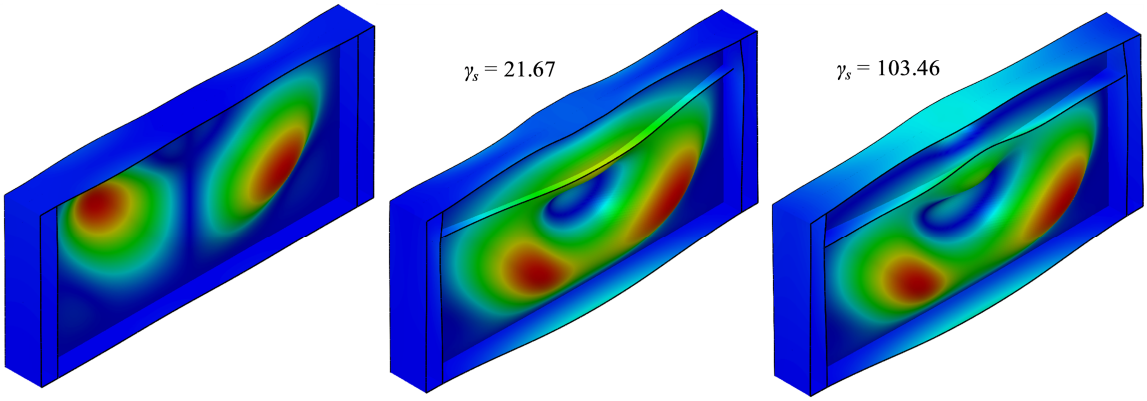

Figure 8: Third buckling mode of longitudinally unstiffened (valid for $s_s/h_w \leq 0.50$) and stiffened steel plate girders (valid for $s_s/h_w \leq 0.25$ for $\gamma_s = 21.67$ and for $s_s/h_w \leq 0.10$ for $\gamma_s = 103.46$).

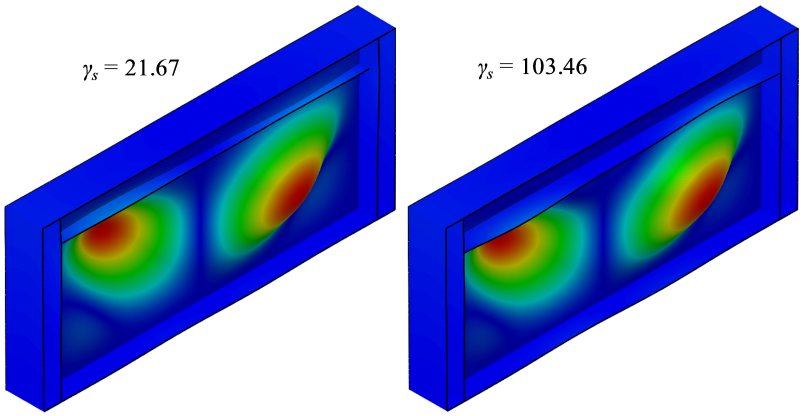

Figure 9: Third buckling mode of longitudinally stiffened steel plate girders valid for $s_s/h_w \geq 0.30$ for $\gamma_s = 21.67$ and $s_s/h_w \geq 0.15$ for $\gamma_s = 103.46$.

Two hand-defined sinusoidal imperfection shapes were also considered; a method of incorporating geometric imperfections employed by (Kovesdi et al. 2018), (Davaine 2005), (Chacon et al. 2009), (Graciano et al. 2011), (Kovesdi 2018), (Loaiza et al. 2018) for I-shaped steel plate girders under patch loading. The hand-defined sinusoidal geometric imperfections considered were represented using sine and cosine functions in both longitudinal and transverse directions (graphically illustrated in Fig. 10), and they can be mathematically described as:

$$\left\{\begin{array}{l} w(x,y) = w_0 \sin\left(\pi x / a\right)\sin\left(\pi y / h_w\right) \\ w(x,y) = \frac{1}{4} w_0 \left(1-\cos\left(2\pi x / a\right)\right)\left(1-\cos\left(2\pi y / h_w\right)\right) \end{array}\right\}, \quad (1)$$

where w_0 is the imperfection amplitude, a is the girder span, and h_w is the web panel depth.

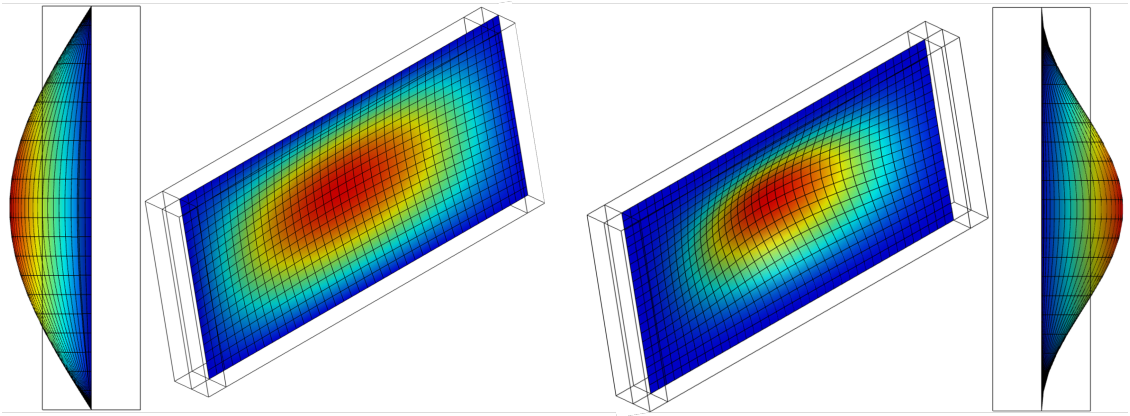

Figure 10: Sine (left) and cosine (right) hand-defined geometric imperfections.

Additionally, the experimentally measured imperfections according to the experimental research (Kovacevic & Markovic 2020) were included in this study as well. The experimental program included 14 tests in total, and initial girder deformations were measured in each test. One such measured initial web panel deformation for longitudinally unstiffened and stiffened plate girders is given in Fig. 11. All 14 initial deformations were considered in the present study.

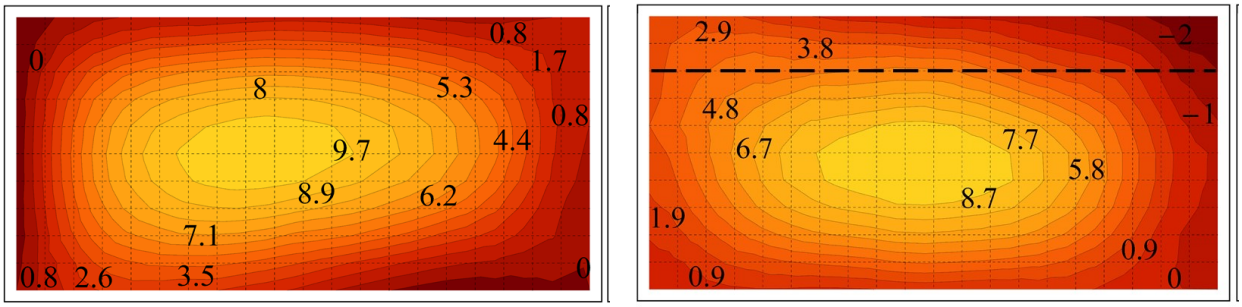

Figure 11: Initial deformation of girder B1 without stiffening (left) and initial deformation of girder B7 with stiffening (right). The dashed line represents the longitudinal stiffener. Refer to (Kovacevic & Markovic 2020) for more details.

The maximum imperfection amplitude was set to be $w_0 = h_w/100$ for all the imperfection shapes considered, as frequently used in similar studies (Chacon et al. 2009), (Graciano et al. 2011), (Kovacevic et al. 2019), (Kovacevic & Markovic 2019).

3. Results and discussion

For the sake of brevity, the computationally obtained patch load resistances of longitudinally unstiffened and stiffened steel plate girders are graphically presented as a function of patch load length and ultimate strength for one representative experimentally measured imperfection (e.g., geometric imperfection shape B2) for each buckling-affine and hand-defined geometric imperfection in Fig. 12, Fig. 13, and Fig. 14, respectively. The interested reader is referred to (Kovacevic et al. 2021b) for all the other geometric imperfections considered.

3.1 Experimentally measured geometric imperfections

The ultimate load of longitudinally stiffened steel plate girders was higher than the carrying capacity of longitudinally unstiffened ones, Fig. 12a; refer to (Kovacevic et al. 2021b) for all the experimentally measured geometric imperfections. This proves to be valid for all the patch load lengths considered, $s_s/h_w \leq 0.50$. Using the relatively weak longitudinal stiffener ($\gamma_s = 21.67$) and for all the experimentally measured imperfections, the strengthening effect for smaller patch load lengths (i.e., $s_s/h_w \leq 0.15$) was <10%, while for longer patch load lengths (i.e., $s_s/h_w = 0.50$) its value was up to 28%. By contrast, using the relatively strong longitudinal stiffener ($\gamma_s = 103.46$) and including all the experimentally measured imperfections, the strengthening effect did not change for smaller patch load lengths (i.e., $s_s/h_w \leq 0.15$), and its contribution was ≤10%. In this case, $\gamma_s = 103.46$, a significant strengthening effect was prominent for longer patch load lengths (i.e., $s_s/h_w = 0.50$), with a maximum value of 48%.

3.2 Buckling mode-affine geometric imperfections

For the first two buckling modes, the following conclusions could be made. The ultimate load of longitudinally stiffened steel plate girders was higher than the ultimate strength of the unstiffened ones (Fig. 12b and Fig. 13a) for all the patch load lengths under consideration, $s_s/h_w \leq 0.50$. For the relatively weak longitudinal stiffener ($\gamma_s = 21.67$), the strengthening effect for smaller patch load lengths (i.e., $s_s/h_w \leq 0.15$) was negligible, while for longer patch load lengths (i.e., $s_s/h_w = 0.50$), the maximum strengthening effect was up to 23% for the first buckling mode and 15% for the second (Fig. 12b and Fig. 13a). In the case of the relatively strong longitudinal stiffener, the strengthening effect for $s_s/h_w \leq 0.10$ can be ignored. In

this case ($\gamma_s = 103.46$), the maximum strengthening effect of 38% was obtained for the second buckling mode (Fig. 13a).

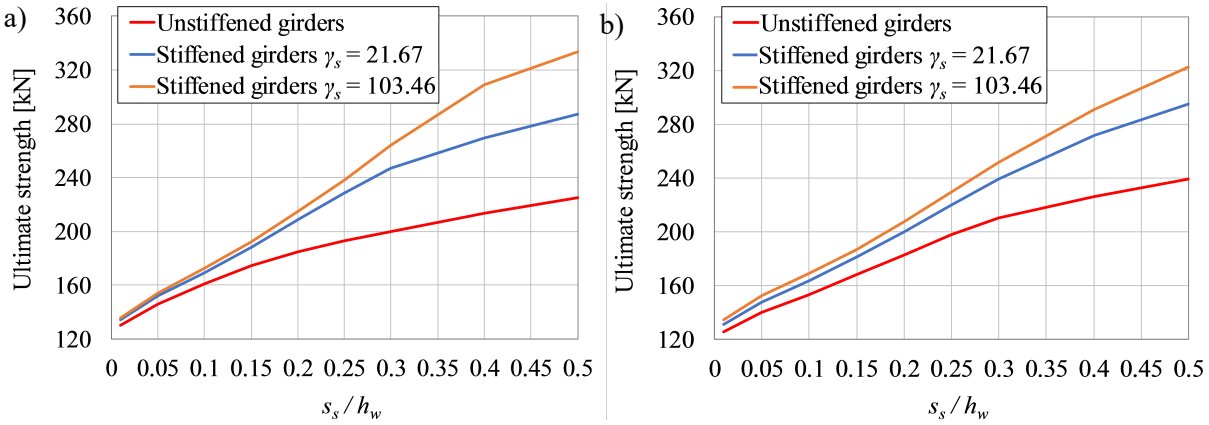

Figure 12: Ultimate strength of longitudinally unstiffened and stiffened steel plate girders using (a) experimentally measured imperfection B2; (b) first buckling mode shape as initial geometric imperfections.

For the third buckling mode, it is apparent that the patch load resistance of longitudinally stiffened steel plate girders was lower than the ultimate load of unstiffened ones for patch load lengths $s_s/h_w \leq 0.20$ and $s_s/h_w \leq 0.10$ for $\gamma_s = 21.67$ and $\gamma_s = 103.46$, respectively (Fig. 13b). The same conclusion was obtained in (Kovacevic et al. 2019) and (Kovacevic & Markovic 2019) (web panel aspect ratio $a/h_w = 1$) for a different patch load length range. The reason lower ultimate strengths of longitudinally stiffened steel plate girders than those of unstiffened ones were returned in this case is directly influenced by the shape of geometric imperfections. The transition patch load lengths at which the carrying capacity of longitudinally stiffened steel plate girders becomes higher than the ultimate load of unstiffened ones (see the increase in the ultimate strength in Fig. 13b) are a consequence of the changed buckling pattern (cf. Fig. 8 and Fig. 9); this is explained in more detail in the next section.

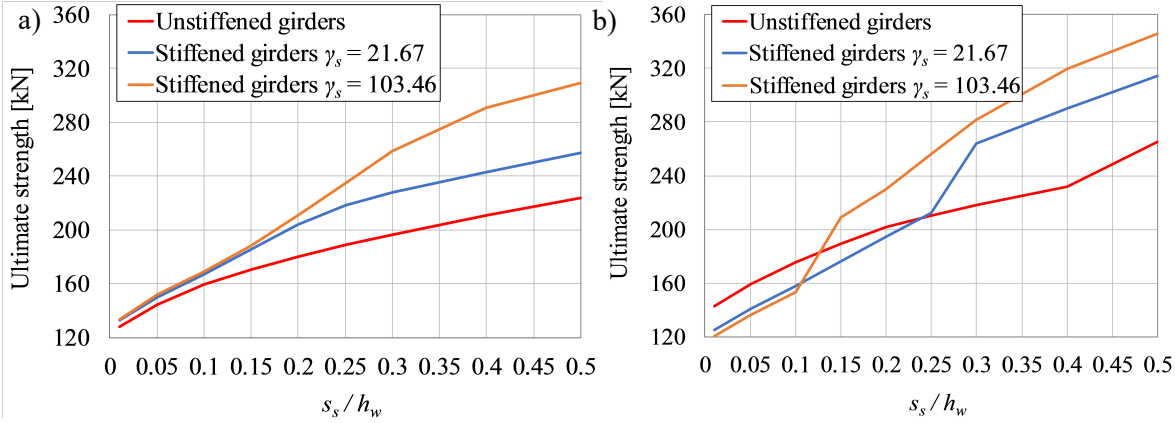

Figure 13: Ultimate strength of longitudinally unstiffened and stiffened steel plate girders using (a) second buckling mode shape; (b) third buckling mode shape as initial geometric imperfections.

3.3 Hand-define sinusoidal geometric imperfections

Finally, considering the hand-defined sinusoidal geometric imperfections (cf. Fig. 10), a similar trend in the results as for the first two buckling modes was observed. In this case, the carrying capacities of longitudinally stiffened steel plate girders were higher than for unstiffened ones for

all the load lengths considered, $s_s/h_w \leq 0.50$, as shown in Fig. 14. For both hand-defined geometric imperfections, the strengthening effect was negligible for $s_s/h_w \leq 0.15$ (valid for both $\gamma_s = 21.67$ and $\gamma_s = 103.46$), while appreciable strengthening effects of 25% and 21% were returned for $s_s/h_w = 0.50$ for the sine and cosine hand-defined geometric imperfections, respectively; significantly larger strengthening effects of 41% and 31% were calculated for $s_s/h_w = 0.50$ and $\gamma_s = 103.46$.

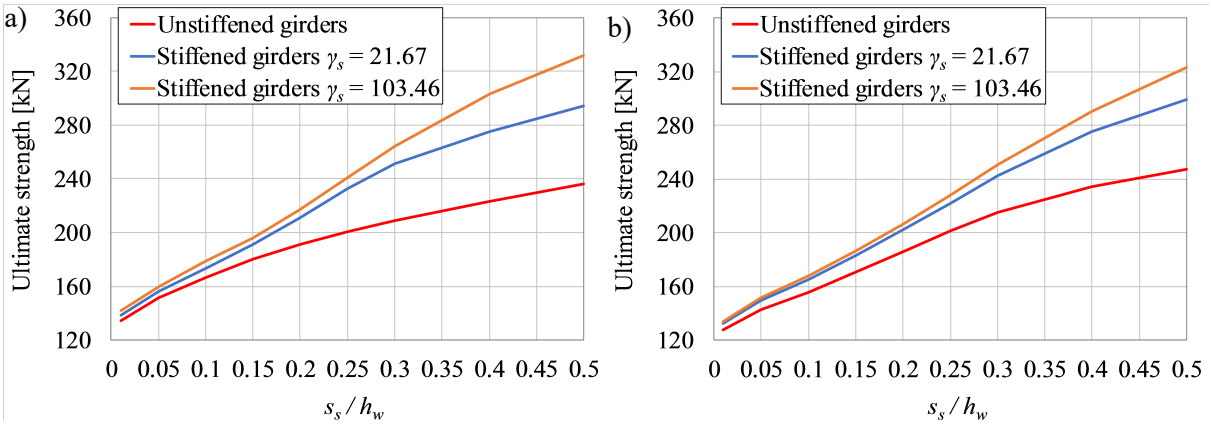

Figure 14: Ultimate strength of longitudinally unstiffened and stiffened steel plate girders using (a) sine hand-defined; (b) cosine hand-defined geometric imperfections.

4. Unfavorable geometric imperfections

In this paper, we sought unfavorable geometric imperfections in steel plate girders under concentrated transverse loading while considering the most often used geometric imperfections for this design case; thus, we are not referring to the worst geometric imperfection, which represents a highly nonlinear optimization problem (Kristanic & Korelc 2008), (Lindgaard et al. 2010). Our goal is to provide broader design guidelines that include a wide range of design situations.

As one can see in Fig. 12, Fig. 13, and Fig. 14, the lowest patch load resistance of longitudinally unstiffened steel plate girders was returned for some experimentally measured and first two buckling mode-affine geometric imperfections; refer to (Kovacevic et al. 2021b) for all numerically obtained ultimate strengths. The actual minimum value is a function of patch load length and differs between these imperfections. For example, for patch load lengths $s_s/h_w \leq 0.15$, the lowest carrying capacity is for experimentally measured geometric imperfection B1. In contrast, for applied load lengths $s_s/h_w \geq 0.20$, the minimum ultimate load is for the second buckling mode-affine geometric imperfection. The same conclusion, that the lowest patch load resistance was computed for the second buckling mode shape for $s_s/h_w \geq 0.20$, was also reported in (Kovacevic et al. 2019) and (Kovacevic & Markovic 2019) for steel plate girders with a web panel aspect ratio $a/h_w = 1$ and in (Chacon et al. 2009) for a constant patch load length ($s_s/h_w = 0.30$) and $a/h_w = 1.50$.

On the other hand, the lowest ultimate strength of longitudinally stiffened steel plate girders ($\gamma_s = 21.67$) was obtained for experimentally measured geometric imperfection B1 and third buckling mode-affine imperfections ($s_s/h_w \leq 0.25$), and the second buckling mode-affine imperfections ($s_s/h_w \geq 0.30$). These findings are in agreement with (Kovacevic et al. 2019) and (Kovacevic & Markovic 2019) (web panel aspect ratio $a/h_w = 1$), in which the transition patch

load length that changed the unfavorable geometric imperfection from the third to the second buckling mode-affine imperfection was at $s_s/h_w = 0.40$. This transition in the unfavorable geometric imperfection from the third to the second buckling mode-affine imperfection is a direct consequence of the buckling pattern change (as shown in Fig. 8 and Fig. 9). For the $\gamma_s = 103.46$ case, the lowest ultimate loads were evaluated for the third buckling mode-affine ($s_s/h_w \leq 0.10$) or for experimentally measured geometric imperfection B1 for patch load lengths $s_s/h_w \geq 0.15$. Similarly, the authors in (Graciano et al. 2011) showed that the lowest ultimate strength of longitudinally stiffened steel plate girders under a constant patch load length ($s_s/h_w = 0.04$) was determined for the third buckling mode-affine imperfection with imperfection amplitudes $w_0 \leq h_w/100$ and positions of the longitudinal stiffener $b_1/h_w \leq 0.25$.

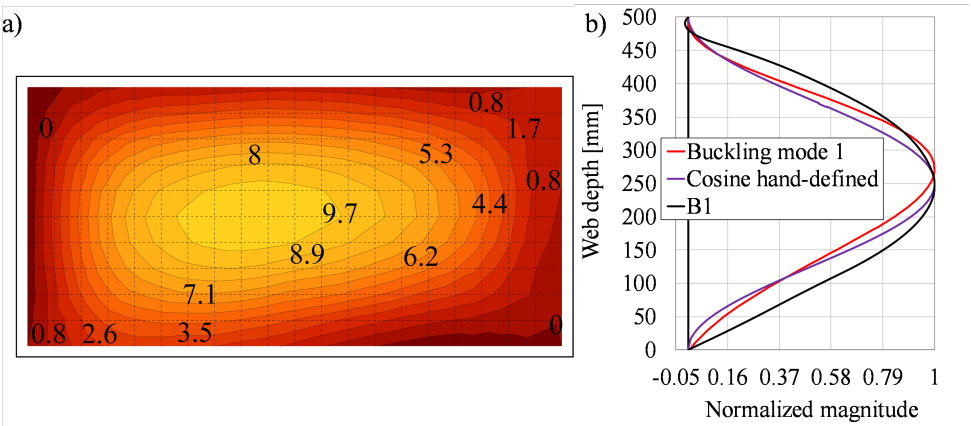

Figure 15: (a) Contour plot of experimentally measured geometric imperfection B1; (b) center line cross-section of the first buckling mode-affine (unstiffened girders), cosine hand-defined, and experimentally measured geometric imperfection B1 (right).

The findings above demonstrate that unfavorable geometric imperfections are dependent on patch load length – that is, a specific geometric imperfection can yield the lowest patch load resistance for a particular patch load length range, which does not need to hold for other patch load lengths. In addition, as explained later in this section, unfavorable geometric imperfections are also dependent on the relative stiffness of the longitudinal stiffener, meaning that different geometric imperfection shapes can lead to the lowest patch load resistance for different relative stiffnesses. Based on the discussion above, the lowest ultimate strengths given in this study were obtained for the buckling mode-affine or experimentally measured geometric imperfection B1. For further discussion in this section and to provide more general conclusions, two cases are considered. The first case is for a relatively small patch load length, $s_s/h_w = 0.10$, and the second one is for a relatively long load length, $s_s/h_w = 0.30$. For the former, the unfavorable geometric imperfection is experimentally measured geometric imperfection B1 (for unstiffened and stiffened steel plate girders $\gamma_s = 21.67$) and the third buckling mode-affine imperfection (for stiffened steel plate girders $\gamma_s = 103.46$). For the second case ($s_s/h_w = 0.30$), the unfavorable geometric imperfection is the second buckling mode-affine imperfection (for unstiffened and stiffened steel plate girders $\gamma_s = 21.67$) and experimentally measured geometric imperfection B1 (Fig. 15a).

Center line cross-sections of the first three buckling mode-affine imperfections, along with corresponding failure modes at collapse for both cases considered ($s_s/h_w = 0.10$ and $s_s/h_w = 0.30$),

are provided in Fig. 16 and Fig. 17. For the sake of brevity, out-of-plane displacements and failure mechanisms for longitudinally unstiffened and stiffened steel plate girders at ultimate load level for both cases considered ($s_s/h_w = 0.10$ and $s_s/h_w = 0.30$), obtained only using the first buckling mode-affine geometric imperfections, are given in Fig. 18 and Fig. 19. As can be observed, the first buckling mode shape of longitudinally unstiffened and stiffened steel plate girders subjected to patch loading resembled a C-shaped initial deformation (one global buckle along the girder depth), as shown in Fig. 16 and Fig. 17. The shape and position of the maximum amplitude of this buckling mode shape were very similar for both longitudinally unstiffened and stiffened steel plate girders (the maximum amplitude is pronounced in the lower part of the web). An S-shaped deformation (one local buckle in the upper web sub-panel and an opposite buckle in the lower web sub-panel) was returned at collapse (local failure mode) for both longitudinally unstiffened and stiffened steel plate girders for $\gamma_s = 21.67$ and $\gamma_s = 103.46$, as shown in Fig. 16 and Fig. 18 for loading lengths $s_s/h_w = 0.10$. The failure mechanism was located in the upper part of the web panel (longitudinally unstiffened steel plate girders), and between the loaded flange and longitudinal stiffener for stiffened ones, Fig. 18. Similar out-of-plane displacements were computed for all three girders in Fig. 18 and with similar values for these displacements in the upper part of the web panel; thus, small load lengths had a low impact on the patch loading resistance regardless of the longitudinal stiffener's relative stiffness. A similar S-shaped deformation at collapse was also obtained for longer patch load lengths ($s_s/h_w = 0.30$) but with less pronounced deformation in the upper web sub-panel, as shown in Fig. 17 and Fig 19. In this case ($s_s/h_w = 0.30$), out-of-plane displacements differed for all three girders in Fig. 19 and they were significantly lower than in the first case $s_s/h_w = 0.10$ (cf. Fig. 18). Hence, using the first buckling mode-affine geometric imperfection returned an S-shaped deformation at collapse regardless of the relative stiffness for both cases ($s_s/h_w = 0.10$ and $s_s/h_w = 0.30$) but with different amount of pronounced deformation in the upper part of the web panel.

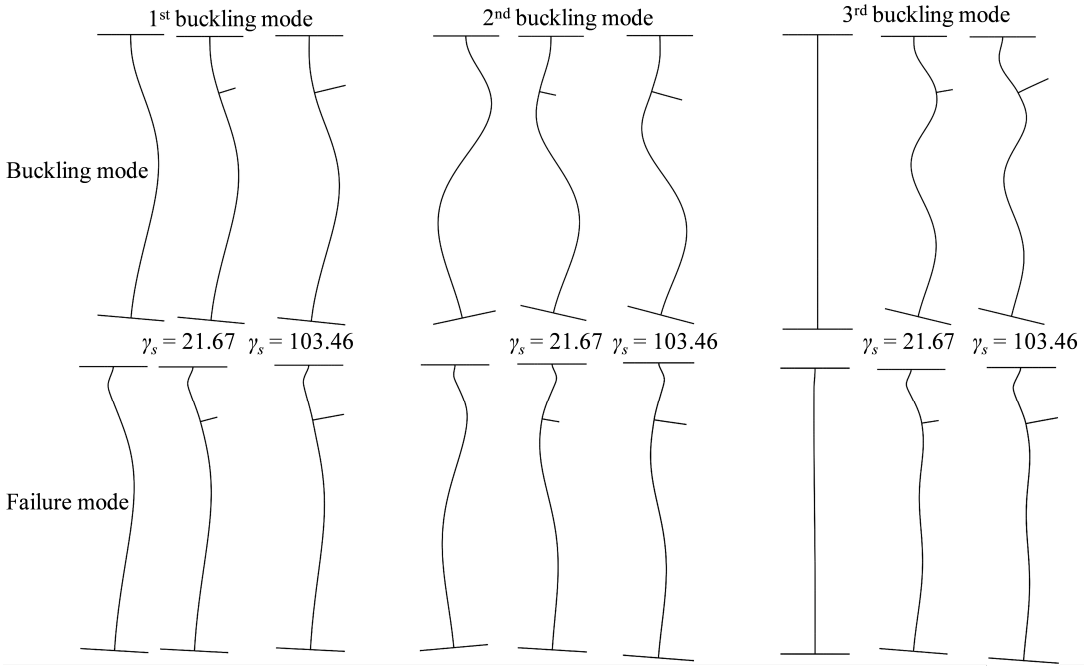

Figure 16: Center line cross-section of the first three buckling mode-affine geometric imperfections (magnified 50 times) and corresponding failure modes at collapse (magnified 5 times) for longitudinally unstiffened and stiffened steel plate girders for $s_s/h_w = 0.10$.

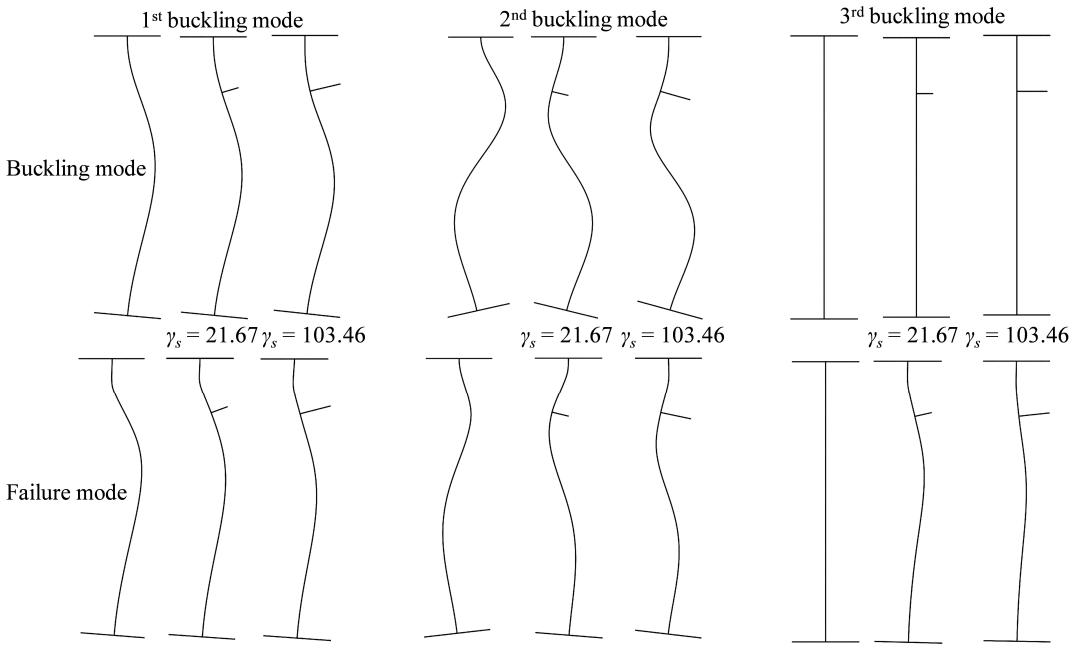

Figure 17: Center line cross section of the first three buckling mode-affine geometric imperfections (magnified 50 times) and corresponding failure modes at collapse (magnified 5 times) for longitudinally unstiffened and stiffened steel plate girders for $s_s/h_w = 0.30$.

The second buckling mode of both groups of steel plate girders returned an S-shaped initial deformation, as shown in Fig. 7, Fig. 16, and Fig. 17. However, the position and maximum amplitude of this initial deformation differed between longitudinally unstiffened and stiffened steel plate girders. For longitudinally unstiffened steel plate girders, the maximum amplitude was equally pronounced in the upper and lower part of the web panel. By contrast, the position of the maximum amplitude for longitudinally stiffened steel plate girders ($\gamma_s = 21.67$ and $\gamma_s = 103.46$) was dominant in the lower web sub-panel, whereas slight deformation was also present in the upper web sub-panel and at the longitudinal stiffener position. As shown in Fig. 16 and Fig. 17, similar failure shapes at collapse were returned with pronounced deformations at the longitudinal stiffener position and in the upper web sub-panel.

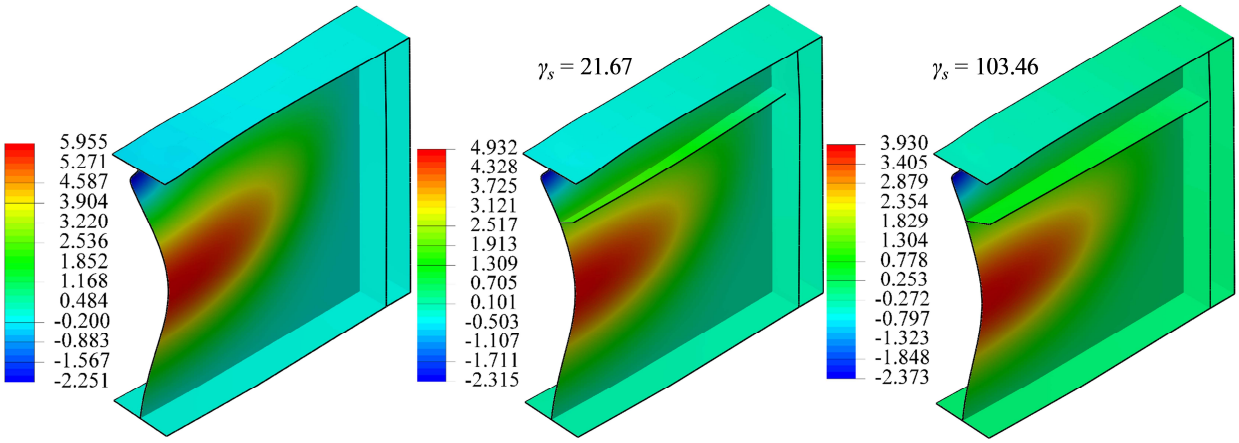

Figure 18: Out-of-plane displacement (units are in mm) and failure mechanism for longitudinally unstiffened and stiffened steel plate girders at ultimate load level for $s_s/h_w = 0.10$. The first buckling mode-affine geometric imperfections are employed. Deformation is magnified 10 times.

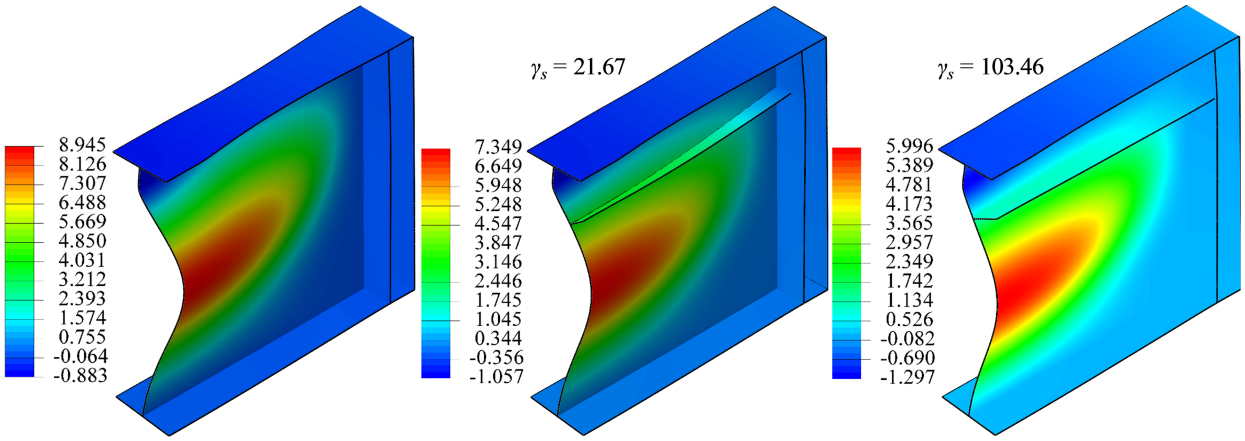

Figure 19: Out-of-plane displacement (units are in mm) and failure mechanism for longitudinally unstiffened and stiffened steel plate girders at ultimate load level for $s_s/h_w = 0.30$. The first buckling mode-affine geometric imperfections are employed. Deformation is magnified 10 times.

As can be observed considering the third buckling mode shape of longitudinally unstiffened and stiffened steel plate girders (cf. Fig. 8 and Fig. 9), the shape and position of the maximum amplitude for this geometric imperfection were very different between longitudinally unstiffened and stiffened plate girders. Asymmetric buckling mode shapes were obtained for longitudinally unstiffened steel plate girders (for all load lengths $s_s/h_w \leq 0.50$) with no deformation directly below the applied load. Therefore, the highest ultimate strengths for longitudinally unstiffened steel plate girders were determined by juxtaposing all the geometric imperfections considered (except for some extreme values for experimentally measured imperfections for patch load lengths $s_s/h_w = 0.30$ and $s_s/h_w = 0.40$). For longitudinally stiffened steel plate girders ($\gamma_s = 21.67$ and $\gamma_s = 103.46$) and small patch load lengths $s_s/h_w = 0.10$, a significant, pronounced initial deformation was dominant in the upper web sub-panel and at the stiffener position, as shown in Fig.8 and Fig. 16. By contrast, for $s_s/h_w = 0.30$, asymmetric mode shapes were returned with no deformation directly below the applied load (Fig. 9 and Fig. 17), which in turn, produced noticeably higher ultimate strengths of longitudinally stiffened steel plate girders.

Examining the failure mode shapes at collapse for $s_s/h_w = 0.10$ (cf. Fig. 16), the following conclusions could be drawn. All failure mode shapes in Fig. 16 showed pronounced deformation directly below the loaded flange in the upper web sub-panel or at the stiffener location (except for the asymmetrical third buckling mode of longitudinally unstiffened steel plate girders), although geometric imperfections were different, Fig. 20. The only buckling mode shape that had pronounced deformation directly under the loaded flange was the third buckling mode shape of longitudinally stiffened steel plate girders ($\gamma_s = 103.46$). Indeed, the lowest patch load resistances were determined for these steel plate girders using the third buckling mode-affine imperfections for the case $s_s/h_w = 0.10$. The buckling mode shapes of longitudinally unstiffened and stiffened steel plate girders ($\gamma_s = 21.67$) did not show pronounced deformation close to the loaded flange. As shown in Fig.15b, experimentally measured geometric imperfection B1 was very similar to the first buckling mode shape. However, imperfection shape B1 had a small deformation very close to the loaded flange compared to the first buckling mode shape, and thus, the lowest ultimate strengths were obtained for this geometric imperfection for both longitudinally unstiffened and stiffened steel plate girders, $\gamma_s = 21.67$ for $s_s/h_w = 0.10$.

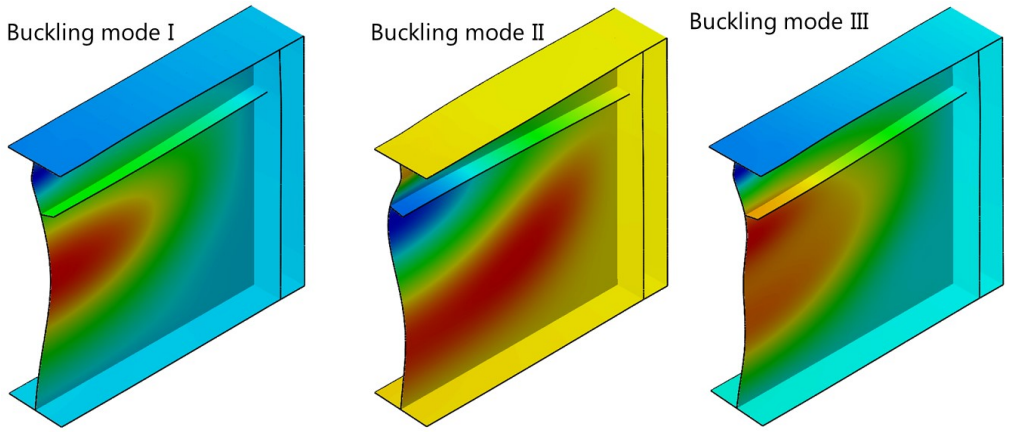

Figure 20: Failure mode at collapse for longitudinally stiffened steel plate girders ($\gamma_s = 21.67$) for $s_s/h_w = 0.10$ for various geometric imperfections. The deformation is magnified five times.

Similar conclusions can be drawn from the failure mode shapes in Fig. 17 for longer patch load length $s_s/h_w = 0.30$. Again, very similar failure mode shapes were returned for both longitudinally unstiffened and stiffened steel plate girders (apart from the third buckling mode-affine imperfections—asymmetric buckling mode), although initial geometric imperfections were different, Fig. 21. The second buckling mode shape of longitudinally unstiffened steel plate girders resembled the failure mode at collapse, and hence, the lowest ultimate strengths were determined for this geometric imperfection. The same observation was noted for longitudinally stiffened steel plate girders ($\gamma_s = 21.67$) since the longitudinal stiffener was relatively weak. For the much stronger longitudinal stiffener ($\gamma_s = 103.46$), the first three buckling mode shapes did not resemble the failure mode at collapse (the closest one was the first buckling mode shape), as shown in Fig. 17. In this case, for $\gamma_s = 103.46$, the failure mode at collapse showed small deformations below the loaded flange and at the stiffener position, while for $\gamma_s = 21.67$, a significantly larger deformation formed at the stiffener position (weak stiffener). The failure mode at collapse is governed by the relative stiffness of the longitudinal stiffener, γ_s, which in turn requires a different initial geometric imperfection shape to resemble the failure mode shape. In this case, $\gamma_s = 103.46$, the lowest carrying capacities were computed for experimentally measured geometric imperfection B1, which indeed showed a small deformation close to the loaded flange, as shown in Fig.15b.

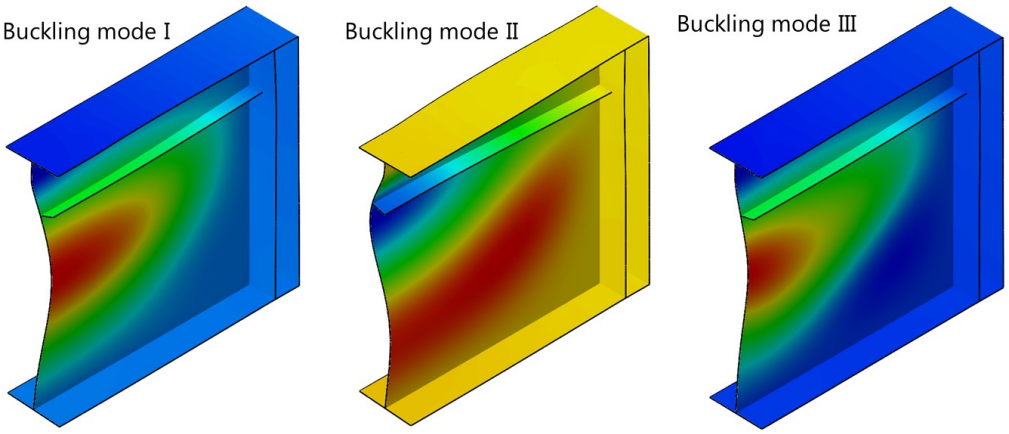

Figure 21: Failure mode at collapse for longitudinally stiffened steel plate girders ($\gamma_s = 21.67$) for $s_s/h_w = 0.30$ for various geometric imperfections. The deformation is magnified five times.

The conclusions above demonstrate that the process of defining unfavorable geometric imperfections in steel plate girders subjected to patch loading is governed by the patch load length and the relative stiffness of the longitudinal stiffener. One can determine different unfavorable geometric imperfections for different values of the patch load length and the longitudinal stiffener's relative stiffness (under a constant imperfection amplitude). As shown in this paper, the lowest patch load resistances were returned for geometric imperfections that resembled the deformation at collapse. This finding was also proved in (Kovacevic et al. 2019) comparing the deformed shaped at collapse obtained experimentally with the third buckling mode (the geometric imperfection that returned the lowest ultimate strength) of steel plate girder with $s_s/h_w = 0.20$, Fig. 22.

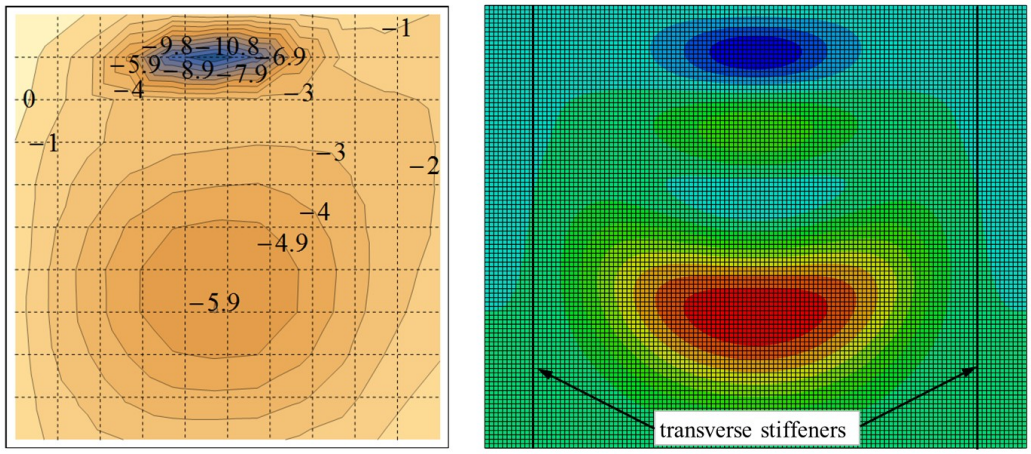

Figure 22: Deformed shape at collapse (units are in mm) obtained experimentally in (Markovic & Kovacevic 2019) (left) and third buckling mode (right) for steel plate girder with $s_s/h_w = 0.2$.

The concept of collapse-affine geometric imperfections seems impractical for design purposes since a geometrically and materially nonlinear analysis must be conducted before collapse-affine geometric imperfection shapes are determined. However, to be safe, designers can employ this concept of collapse-affine geometric imperfections instead of buckling mode-affine geometric imperfections (as recommended in (EN 1993-1-5 2006)), as these collapse-affine geometric imperfections lead to lower ultimate strengths than those given by buckling modes.

4. Conclusions

The present finite element parametric study was designed to determine the influence of various geometric imperfections (in combination with a variety of patch load lengths) on the patch load resistance of I-shaped steel plate girders. Experimentally measured, buckling mode-affine, and hand defined sinusoidal geometric imperfections were varied in the study in combination with varying patch load lengths and relative stiffnesses of the longitudinal stiffener.

The ultimate strength of longitudinally unstiffened and stiffened steel plate girders increases as the patch load length increases. This was shown to be valid for all the geometric imperfections considered. For very small patch load lengths (i.e., $s_s/h_w < 0.15$), the ultimate strength of longitudinally stiffened steel plate girders follows the ultimate load of unstiffened ones regardless of the relative stiffness of the longitudinal stiffener and the geometric imperfection; hence, the strengthening effect is negligible (less than 10%).

We showed that geometric imperfections can play a decisive role and significantly affect the ultimate strength of longitudinally unstiffened and stiffened steel plate girders. Unfavorable geometric imperfections in steel plate girders subjected to patch loading are governed by the patch load length and the relative stiffness of the longitudinal stiffener. One can identify different unfavorable geometric imperfections for different values of the patch load length and the relative stiffness of the longitudinal stiffener (under a constant imperfection amplitude).

As shown in this paper, the lowest patch load resistances were returned for geometric imperfections that resembled the deformation at collapse (collapse-affine imperfections). For safety, designers can employ this concept of collapse-affine geometric imperfections instead of buckling mode-affine geometric imperfections (as recommended in the current European design standard). In order to simplify the applicability of the collapse-affine imperfection concept, further research should focus on finding an *equivalent shape* that resembles the deformation at failure for different patch load lengths and girder characteristics, such as the relative stiffness of the longitudinal stiffener, web slenderness, et cetera.

Geometric imperfections that have pronounced deformations directly under the loaded flange lead to lower load resistances regardless of the longitudinal stiffener relative stiffness and small patch load lengths ($s_s/h_w \leq 0.10$). These local geometric imperfections in the upper web sub-panel yield lower ultimate strengths than those defined over the whole web depth (global geometric imperfections). This conclusion was also found to be valid for longitudinally stiffened steel plate girders reinforced by relatively strong longitudinal stiffeners and longer patch load lengths, such as $s_s/h_w = 0.30$. For longitudinally stiffened steel plate girders reinforced by relatively weak longitudinal stiffeners and under longer patch load lengths ($s_s/h_w = 0.30$), geometric imperfections defined in the upper web sub-panel and at the stiffener location (combined geometric imperfections) lead to lower ultimate strengths than global geometric imperfections.

References

Abaqus Simulia. (2016). Dassault Systemes.

ANSI/AISC. (2016). Specification for Structural Steel Buildings. Chicago, Illinois: American Institute of Steel Construction.

Bergfelt, A. (1983). "Girder web stiffening for patch loading." Department of Structural Engineering. Chalmers University of Technology.

Chacon, R., Mirambell, E., Real, E. (2009). "Influence of designer-assumed initial conditions on the numerical modelling of steel plate girders subjected to patch loading." *Thin-Walled Structures,* 47 391-402.

Chacon, R., Serrat, M., Real, E. (2012). "The influence of structural imperfections on the resistance of plate girders to patch loading." *Thin-Walled Structures,* 53 15-25.

Cooper, P. (1965). "Bending and shear strength of longitudinally stiffened plate girders." Doctoral thesis. Fritz Laboratory Reports.

Demari, F.E., Mezzomo, G.P., Pravia, Z.M.C. (2020). "Numerical study of slender I-girders with one longitudinal stiffener under patch loading." *Journal of Constructional Steel Research,* 167 105964.

Davaine, L. (2005). "Formulation de la résistance au lancement d'une âme métallique de pont raidie longitudinalement." Doctoral thesis. Rennes, France: INSA.

EN 1993-1-5:2005 (2006) Eurocode 3: Design of Steel Structures. Part 1-5: Plated Structural Elements. CEN

Graciano, C., Casanova, E., Martinez, J. (2011). "Imperfection sensitivity of plate girder webs subjected to patch loading." *Journal of Constructional Steel Research,* 67 1128-1133.

Hajdin, N., Markovic, N., Kovacevic, S. (2019). "Patch load on longitudinally stiffened plate girders." *Proceedings of the 10th International Conference on Bridges in Danube Basin,* Vienna, Austria. 140-143

Janus, K., Karnikova, I., Skaloud, M. (1988). “Experimental investigation into the ultimate load behavior of longitudinally stiffened steel webs under partial edge loading.” *Acta Tech. CSAV,* 2 158-195.
Kovacevic, S., Markovic, N. (2019). “Influence of the length of patch load on the ultimate load of longitudinally stiffened plate girders.” *Proceedings of the Annual Stability Conference, Structural Stability Research Council (SSRC),* St. Louis, MO.
Kovacevic, S., Markovic, N. (2020). “Experimental study on the influence of patch load length on steel plate girders.” *Thin-Walled Structures,* 151 106733.
Kovacevic, S., Ceranic, A., Markovic, N., Bendic, M. (2021a). “Patch load resistance of longitudinally stiffened steel plate girders: A parametric study.” *Proceedings of the 9th European Conference on Steel and Composite Structures (Eurosteel 2021),* Sheffield, UK.
Kovacevic, S., Markovic, N., Sumarac, D., Salatic, R. (2019). “Influence of patch load length on plate girders. Part II: Numerical research.” *Journal of Constructional Steel Research,* 158 213-229.
Kovacevic, S., Markovic, N., Sumarac, D., Salatic, R. (2021b). “Unfavorable geometric imperfections in steel plate girders subjected to localized loads.” *Thin-Walled Structures,* 161 107412.
Kovesdi, B. (2018). “Patch loading resistance of slender plate girders with longitudinal stiffeners.” *Journal of Constructional Steel Research,* 140 237-246.
Kovesdi, B., Mecseri, B.J., Dunai, L. (2018). “Imperfection analysis on the patch loading resistance of girders with open section longitudinal stiffeners.” *Thin-Walled Structures,* 123 195-205.
Kristanic, N., Korelc, J. (2008). “Optimization method for the determination of the most unfavorable imperfection of structures.” *Computational Mechanics,* 42 859-872.
Lindgaard, E., Lund, E., Rasmussen, K. (2010). “Nonlinear buckling optimization of composite structures considering ‘worst’ shape imperfections.” *International Journal of Solids and Structures,* 47 3186-3202.
Loaiza, N., Graciano, C., Casanova, E. (2018). “Design recommendations for patch loading resistance of longitudinally stiffened I-girders.” *Engineering Structures,* 171 747-758.
Markovic, N. (2003). “Buckling of plate girders under the action of patch loading.” Doctoral thesis (in Serbian). University of Belgrade, Serbia.
Markovic, N., Hajdin, N. (1992). “A contribution to the analysis of the behavior of plate girders subjected to patch loading.” *Journal of Constructional Steel Research,* 21 163-173.
Markovic, N., Kovacevic, S. (2019). “Influence of patch load length on plate girders. Part I: Experimental research.” *Journal of Constructional Steel Research,* 157 207-228.
Riks, E. (1979). “An incremental approach to the solution of snapping and buckling problems.”International Journal of Solids and Structures*,* 15 529-551.